

Rhabdoid tumor: gene expression clues to pathogenesis and potential therapeutic targets

Samantha Gadd^{1,2,4}, Simone Treiger Sredni^{1,2,4}, Chiang-Ching Huang^{2,3}, Elizabeth J Perlman^{1,2} and the Renal Tumor Committee of the Children's Oncology Group

Rhabdoid tumors (RT) are aggressive tumors characterized by genetic loss of *SMARCB1* (*SNF5*, *INI-1*), a component of the SWI/SNF chromatin remodeling complex. No effective treatment is currently available. This study seeks to shed light on the *SMARCB1*-mediated pathogenesis of RT and to discover potential therapeutic targets. Global gene expression of 10 RT was compared with 12 cellular mesoblastic nephromas, 16 clear cell sarcomas of the kidney, and 15 Wilms tumors. In all, 114 top genes were differentially expressed in RT ($P < 0.001$, fold change > 2 or < 0.5). Among these were down-regulation of *SMARCB1* and genes previously associated with *SMARCB1* (*ATP1B1*, *PTN*, *DOCK4*, *NQO1*, *PLOD1*, *PTP4A2*, *PTPRK*); 28/114 top differentially expressed genes were involved with neural or neural crest development and were all sharply downregulated. This was confirmed by Gene Set Enrichment Analysis (GSEA). Neural and neural crest stem cell marker proteins SOX10, ID3, CD133, and Musashi were negative by immunohistochemistry, whereas Nestin was positive. Decreased expression of *CDKN1A*, *CDKN1B*, *CDKN1C*, *CDKN2A*, and *CCND1* was identified, while *MYC-C* was upregulated. GSEA of independent gene sets associated with bivalent histone modification and polycomb group targets in embryonic stem cells showed significant negative enrichment in RT. Several differentially expressed genes were associated with tumor suppression, invasion, and metastasis, including *SPP1* (osteopontin), *COL18A1* (endostatin), *PTPRK*, and *DOCK4*. We conclude that RTs arise within early progenitor cells during a critical developmental window in which loss of *SMARCB1* directly results in repression of neural development, loss of cyclin-dependent kinase inhibition, and trithorax/polycomb dysregulation.

Laboratory Investigation (2010) 90, 724–738; doi:10.1038/labinvest.2010.66; published online 8 March 2010

KEYWORDS: gene expression; rhabdoid tumor; pediatric renal tumors; neural crest; INI-1; SMARCB1

Rhabdoid tumors (RT) are highly malignant neoplasms first described in the kidney of young children. RTs also arise in a variety of extra-renal sites including soft tissues and the central nervous system, where they are often called atypical-teratoid/RT.^{1–3} RTs at all sites have a common genetic abnormality, the mutation or deletion of the *SMARCB1/hSNF5/INI-1* gene located at chromosome 22q11.^{3–5} This gene, which will be referred to as *SMARCB1*, encodes a component of the SWI/SNF chromatin remodeling complex that has an important role in transcriptional regulation (reviewed in Imbalzano and Jones⁶). This has resulted in considerable scientific attention to RTs in recent years, as they represent a potent model for the investigation of this important chromatin remodeling complex. Clinically, over 70% of children with RT present with non-localized disease, and

chemotherapy alone is rarely curative.¹ With an overall survival of 23%, new therapeutic options are needed. The overall goals of this study are to identify genetic pathways that will clarify the nature of RTs and to identify therapeutic targets.

MATERIALS AND METHODS

Patient Samples

Frozen tissue samples were obtained from the Renal Tumor Bank of the Children's Oncology Group. Specimens showing $< 80\%$ tumor cellularity on frozen sections were excluded. A total of 53 tumors were analyzed: 10 RT, 12 cellular mesoblastic nephromas (CMN), 16 clear cell sarcomas of the kidney (CCSK), 15 favorable histology blastemal predominant Wilms tumors (WT). These samples were previously examined for the purpose of developing diag-

¹Department of Pathology, Northwestern University's Feinberg School of Medicine, Chicago, IL, USA; ²Robert H. Lurie Cancer Center, Chicago, IL, USA and ³Department of Preventive Medicine, Northwestern University's Feinberg School of Medicine, Chicago, IL, USA

Correspondence: EJ Perlman, MD, Pathologist-in-Chief, Children's Memorial Hospital, 2300 Children's Plaza, Box 17, Chicago, IL 60614, USA.

E-mail: eperlman@childrensmemorial.org

⁴These two authors contributed equally to the manuscript and project.

Received 20 March 2009; revised 27 November 2009; accepted 17 December 2009

nostic signatures.⁷ Relatively equal numbers of tumors from each category were analyzed so that no single group biased the statistical analysis. All RT demonstrated loss of nuclear staining for BAF47, the protein encoded by *SMARCB1*,⁸ and all cellular CMNs demonstrated the ETV6-NTRK3 fusion transcript characteristic of this entity.⁹ Two fetal kidneys (16–18-weeks gestation) were analyzed for comparison.

Gene Expression Analysis

RNA was extracted and hybridized to Affymetrix U133A arrays (Affymetrix, Santa Clara, CA, USA), scanned, and subjected to quality control parameters and normalization as described earlier.⁷ The gene expression of RT was compared with the other tumor types using two-sample *t*-tests. Affymetrix NetAffx Analysis Center was used to categorize genes and to establish the chromosomal location of differentially expressed genes. Two bioinformatics tools were used to analyze the data, Protein ANalysis THrough Evolutionary Relationships (PANTHER), and Gene Set Enrichment Analysis (GSEA). PANTHER classifies genes by their functions using published experimental evidence, and these are grouped into families and subfamilies of shared function. The detection of significant over- or under-represented functional pathways in a preselected gene list is determined by the binomial test. The Bonferroni-corrected *P*-values are calculated to adjust for multiple testing.¹⁰ GSEA contains gene sets that relate to common biological function, including those from Gene Ontology groups as well as curated gene lists from different pathways and publications. GSEA first ranks the expression of each gene based on its correlation with one of two phenotypes being compared (in this case RT vs non-RT). It then identifies this rank position within the independent gene set being queried. From this ranking it calculates an enrichment score that reflects the degree to which genes within the independent gene set are over represented within those genes most highly correlating with one of the two phenotypes. The normalized enrichment score (NES) takes into account the number of genes within the independent gene set. Permutation on the phenotype class labels is used to obtain the null distribution of NES and the nominal *P*-value. The false discovery rate (FDR) is computed by comparing the tails of the observed and null distributions for the NES (<http://www.broadinstitute.org/gsea>).¹¹

Real-Time Quantitative RT-PCR

TaqMan Gold and the ABI Prism 7700 Sequence Detection System (Applied Biosystems, Foster City, CA, USA) were used. RT-PCR cycle parameters were 48°C for 30 min, 95°C for 15 min, followed by 40 cycles at 95°C for 15 s, and 59°C for 1 min. Sequences of probes and primers are shown in Table 1. Each threshold cycle (C_T) was determined and the C_T for the housekeeping gene (β -actin or GAPDH) was subtracted from this for normalization (dC_T).

Immunohistochemistry

Formalin-fixed-paraffin-embedded tissue from six of each RT, CCSK, CMN, and WT were tested using the monoclonal antibodies provided in Table 1. This was visualized by a streptavidin–biotin system (Vectastain Elite ABC kit, Vector Laboratories) followed by ImmunoPure Metal Enhanced DAB Substrate (Thermo Scientific, Rockford, IL, USA) and counter-stained with hematoxylin.

Immunoblotting

Three frozen CCSKs, CMNs, RTs, and WTs were homogenized in sample buffer [0.125 mol/l Tris–HCl (pH, 6.8), 2% SDS, 10% glycerol, 0.001% bromophenol blue, and 5% β -mercaptoethanol]. Equal amounts of protein lysate were run on polyacrylamide SDS gels and transferred to a nitrocellulose membrane (neural cell adhesion molecule (NCAM), CDH2, LGALS1) or PVDF (Immobilon-P) membrane (TFRC, CMYC). Membranes were blocked and incubated overnight at 4°C in primary antibody (provided in Table 1). The washed membranes were incubated with alkaline phosphatase antimouse IgG (Vector Laboratories), and color was developed with a 5-bromo-4-chloro-3-indolyl phosphate/nitroblue tetrazolium alkaline phosphatase substrate kit IV detection kit (Vector Laboratories).

RESULTS

Overall Differential Gene Expression in RTs

To establish a broad list of probesets containing the majority of genes involved in the pathogenesis of RT, the expression of RT was compared with all the other tumor types combined ('non-RT'), resulting in 2921 probesets with *P*-value < 0.001 and FDR of $\leq 1\%$ (Supplementary Table 1, available at the journal's website). The raw data from this study have been deposited in GEO, accession number GSE11482. To define a more restrictive list of probesets more uniquely expressed in RT, the gene expression of RT was compared with each of the other tumor types separately. Comparing RT to each of these clinically, pathologically, and genetically different tumor categories minimizes erroneous conclusions that may result from a single comparison. Genes present in each one of the resulting four comparisons (RT vs CCSK, RT vs CMN, RT vs WT, and RT vs all non-RT) with a *P*-value of < 0.001 in each are provided in Supplementary Table 2 (426 genes). Of these, 114 genes showed fold change > 2 or < 0.5 in the comparison between RT and all non-RT and are provided in Table 2, arranged in recurring functional groups indicated by GO and PANTHER. The chromosomal location of all probesets in Supplementary Table 1 was analyzed, and no chromosomal arm was over-represented, including probesets on chromosome 22. The 766 genes differentially expressed between RT and non-RT (*P* < 0.0001) were analyzed in PANTHER, and those groups within the biologic process category over-represented with a Bonferroni corrected *P*-value < 0.05 are listed in Supplementary Table 3.

Table 1 Reagents utilized for verification of gene expression*(A) Primers and probes for quantitative RT-PCR*

Gene name	Taqman probe	Forward primer	Reverse primer
SMARCB1	ACCATGACCCAGCTGTGATCCATGAGA	CCTTCCCCCTTTGCTTTGA	GCACCTCGGGCTGAGATG
PTN	CCAAGCCCAAACCTCAAGCAGAATCTAAGA	CAAGCCCTGTGGCAAACCTG	TGTTTCTTGCTTCCTTTTCTTC
FYN	TTCCCAGCAATTATGTGGCTCCAGTTGA	GGAAGCCCGCTCCTTGAC	AAAGTACCACTCTTCTGCTGGATAG
PTPRK	TCAGATCACGACCCTGGAGAAAAGCC	AGATGCCCAAGGTTCTATATG	GTGAGTGTCTTCTCCTTCATTGTAG
NQO1	TGGTCAGAAGGGAATTGCTCAGAGAAGGTAA	TCCAATGTTCTATTAATCACCTCTCTGTA	CTTGTGCTAGGCATATTAGTAAGTCTT
TFRC	ATCCCAGCAGTTTCTTCTGTTTTGCGA	GCTTCCCTTCTTCTGCATATTC	CATGGTGGTACCCAAATAAGGATAA
CCND1	CGGCCTTCCCAGCACCAAC	TGGGTCTGTGCATTCTGGTT	CTTTCATGTTTGTCTTTTGTCTTCTG
β -actin	ATGCCCTCCCCATGCCATCCTGCGT	TCACCCACACTGTGCCATCTACGA	CAGCGGAACCGCTCATTGCCAATGG
GAPDH	AACAGCGACCCACTCCTCCACCTT	AGAAAACTGCCAAATATGATGAC	GTGGTCGTTGAGGGCAATG

(B) Antibodies for immunohistochemistry and immunoblotting

Antibody	Company (city)	Dilution
BAF47 (SMARCB1)	BD Transduction Lab (San Jose, CA, USA)	1/500
NQO1	SigmaAldrich (St Louis, MO, USA)	1/50
CTNNB1	Zymed/Invitrogen	1/200
ID3	Abcam Inc (Cambridge, MA, USA)	1/2
SOX10	SantaCruz (Santa Cruz, CA, USA)	1/50
Musashi	R&D Systems (Minneapolis, MN, USA)	1/200
CD133	Miltenyi Biotec (Auburn, CA, USA)	1/10
Nestin	SantaCruz (Santa Cruz, CA, USA)	1/500
p53	Dako (Carpenteria, CA, USA)	1/100
p21	Dako (Carpenteria, CA, USA)	1/50
p27	Dako (Carpenteria, CA, USA)	1/200
cyclin E	NeoMarkers (Fremont, CA, USA)	1/25
cyclin D1	Dako (Carpenteria, CA, USA)	1/300
PEDF	SantaCruz (Santa Cruz, CA, USA)	1/50
SPP1	Novocastra (Newcastle upon Tyne, UK)	1/100
CDH2	Invitrogen (Carlsbad, CA, USA)	1/100
NCAM	SantaCruz (Santa Cruz, CA, USA)	1/200
LGALS1	Vector Labs (Burlingame, CA, USA)	1/200
CMYC	SantaCruz (Santa Cruz, CA, USA)	1/100
TFRC	Invitrogen (Carlsbad, CA, USA)	1/500

Decreased Expression of SMARCB1 and Associated Genes in Rhabdoid Tumors

SMARCB1 was within the top five genes most significantly differentially expressed in RT, and 12 of the top 114 genes in Table 2 have been shown to be concordantly expressed with *SMARCB1* in prior gene expression analyses. These include genes previously demonstrated to be concordantly differentially expressed after induction of *SMARCB1* within RT cell lines (*ATP1B1*, *PTN*, *SPOCK1*, *DOCK4*, *SERPINE2*), and after inactivation of *SMARCB1* within murine embryonic fibroblasts (*NQO1*, *PLOD1*, *PTP4A2*, *PTPRK*).^{12–14} In addition, Pomeroy *et al* compared RT with four pediatric central nervous system

tumors and provided the top 100 genes characterizing each tumor type. Of the resulting 500 genes, 99 were also found in our Supplementary Table 1 and were concordantly regulated (designated by an asterisk); two genes, *COL5A2* and *RSUI*, were identified in Table 2.¹⁵ Finally, *SPP1* was shown to be significantly upregulated in human RT.¹⁶ The gene expression patterns of *SMARCB1* and selected *SMARCB1*-associated genes are illustrated in Figure 1. The downregulation of *SMARCB1*, *PTN*, and *PTPRK*, and the upregulation of *NQO1* mRNA were confirmed by QRT-PCR (Figure 2). Absence of expression of the *SMARCB1* protein was established in all RTs tested by immunohistochemistry, with strong nuclear positivity identi-

Table 2 Genes with a *P*-value of <0.001 in each comparison of RT vs non-RT, RT vs CMN, RT vs CCSK, RT vs WT, and with a fold change of >2 or <0.5 in the comparison between RT and non-RT

Gene symbol	Description	Chromosome location	UniGene ID	Fold change RT vs non-RT	<i>P</i> -value RT vs non-RT
<i>Genes associated with INI-1</i>					
SMARCB1 ^a	INI-1	22q11	534350	0.49	9.37E-21
ATP1B1	ATPase, Na ⁺ /K ⁺ transporting, β 1 polypeptide	1q24	291196	0.13	3.87E-19
COL5A2	Collagen, type V, α 2	2q14-q32	445827	3.11	1.64E-10
DOCK4 ^{a,b}	Dedicator of cytokinesis 4	7q31.1	654652	0.40	8.11E-20
NQO1	NAD(P)H dehydrogenase, quinone 1	16q22.1	406515	4.58	1.33E-06
PLOD1	Procollagen-lysine 1, 2-oxoglutarate 5-dioxygenase 1	1p36.3-p36.2	75093	2.17	7.27E-11
PTN ^a	Pleiotrophin (heparin-binding growth factor 8)	7q33-q34	371249	0.33	6.74E-12
PTP4A2	Protein tyrosine phosphatase type IVA, member 2	1p35	470477	2.14	7.47E-07
PTPRK ^{a,b}	Protein tyrosine phosphatase, receptor type, K	6q22.2-q22.3	155919	0.22	3.76E-23
RSU1 ^b	Ras suppressor protein 1	10p13	524161	4.99	1.19E-05
SPOCK1 ^a	Sparc/osteonectin, (testican) 1	5q31	654695	0.25	4.85E-14
SPP1 ^b	Secreted phosphoprotein 1 (osteopontin)	4q21-q25	313	5.42	3.50E-07
SERPINE2 ^a	Serpin peptidase inhibitor, clade E, member 2	2q33-q35	38449	0.21	2.63E-09
<i>Neural development</i>					
CDH2	Cadherin 2, type 1, N-cadherin (neuronal)	18q11.2	464829	0.23	3.30E-06
CITED2	Cbp/p300-interacting transactivator, 2	6q23.3	82071	0.47	1.93E-10
CRIM1	Cysteine-rich transmembrane BMP regulator 1	2p21	332847	0.36	3.23E-15
CXCL12	Chemokine (C-X-C motif) ligand 12	10q11.1	522891	0.27	1.14E-15
DPYSL2	Dihydropyrimidinase-like 2	8p22-p21	173381	0.41	1.10E-04
ENC1	Ectodermal-neural cortex	5q12-q13.3	104925	0.27	1.29E-16
FSTL1	Follistatin-like 1	3q13.33	269512	0.29	4.35E-07
FYN	FYN oncogene related to SRC, FGR, YES	6q21	390567	0.34	3.69E-15
HES1	Hairy and enhancer of split 1 (Drosophila)	3q28-q29	250666	0.49	2.97E-07
IGFBP2	Insulin-like growth factor binding protein 2	2q33-q34	438102	0.35	9.35E-08
LAMA4	Laminin, α 4	6q21	654572	0.33	1.12E-05
LAMB1	Laminin, β 1	7q22	650585	0.29	4.15E-10
LEF1	Lymphoid enhancer-binding factor 1	4q23-q25	555947	0.21	8.22E-18
LMO4	LIM domain only 4	1p22.3	436792	0.25	2.38E-16
NAV2	Neuron navigator 2	11p15.1	502116	0.41	1.01E-11
NCAM1	Neural cell adhesion molecule 1	11q23.1	503878	0.29	1.12E-18
NOTCH2	Notch homolog 2 (Drosophila)	1p13-p11	487360	0.40	4.05E-11
RND3	Rho family GTPase 3	2q23.3	6838	0.23	1.13E-12
SOBP	Sine oculis binding protein homolog	6q21	445244	0.33	3.82E-06
SOX11	SRY (sex determining region Y)-box 11	2p25	432638	0.19	2.76E-24
SPON1	Spondin 1, extracellular matrix protein	11p15.2	643864	0.20	4.51E-13
TSPAN5	Tetraspanin 5	4q23	591706	0.37	1.59E-17
<i>MYC-C targets</i>					
ABCE1	ATP-binding cassette, sub-family E, member 1	1q31.2 /// 4q31	571791	2.10	2.08E-08
ACAT1	Acetyl-coenzyme A acetyltransferase 1	11q22.3-q23.1	232375	2.24	8.78E-08
AHCY	S-adenosylhomocysteine hydrolase	20cen-q13.1	-	2.30	1.71E-06

Table 2 Continued

Gene symbol	Description	Chromosome location	UniGene ID	Fold change RT vs non-RT	P-value RT vs non-RT
CORO1C	Coronin, actin-binding protein, 1C	12q24.1	696037	2.25	3.88E-05
CYCS	Cytochrome c, somatic	7p15.2	437060	2.14	7.26E-06
DDX21	DEAD (Asp-Glu-Ala-Asp) box polypeptide 21	10q21	696064	2.66	7.73E-10
ENO2	Enolase 2 (γ , neuronal)	12p13	511915	2.59	1.67E-06
MTHFD2	Methylenetetrahydrofolate dehydrogenase 2	2p13.1	469030	2.40	1.03E-09
MYO1B	Myosin IB	2q12-q34	439620	0.40	1.44E-06
NEFH	Neurofilament, heavy polypeptide 200kDa	22q12.2	198760	2.22	3.09E-07
PAM	Peptidylglycine α -amidating monooxygenase	5q14-q21	369430	0.41	2.29E-08
SLC39A14	Solute carrier family 39, member 14	8p21.3	491232	2.39	1.58E-06
TFRC ^b	Transferrin receptor (p90, CD71)	3q29	529618	3.16	1.53E-09
<i>Tumor suppression, invasion, or metastasis</i>					
COL18A1	Collagen, type XVIII, α 1 (endostatin)	21q22.3	517356	0.41	2.48E-13
MMP12	Matrix metalloproteinase 12	11q22.3	1695	4.07	6.18E-05
NCOA3	Nuclear receptor coactivator 3	20q12	592142	2.43	5.12E-06
SELENBP1	Selenium-binding protein 1	1q21-q22	632460	0.44	9.15E-20
TES	Testis derived transcript (3 LIM domains)	7q31.2	592286	0.41	1.97E-13
ZNF217	Zinc-finger protein 217	20q13.2	155040	2.65	1.51E-05
<i>Transcription regulation</i>					
AFF1	AF4/FMR2 family, member 1	4q21	480190	0.39	7.15E-09
ATF5	Activating transcription factor 5	19q13.3	9754	2.05	2.17E-04
ATXN1	Ataxin 1	6p23	434961	0.44	5.25E-10
BNIP3	BCL2/adenovirus E1B 19kDa interacting protein 3	10q26.3	144873	2.40	1.65E-06
CBX6	Chromobox homolog 6	22q13.1	592201	2.36	1.65E-10
GPR177	G protein-coupled receptor 177	1p31.3	647659	0.37	1.46E-09
GTF3A	General transcription factor IIIA	13q12.3-q13.1	445977	2.02	2.10E-09
HIST1H2BK	Histone cluster 1, H2bk	6p21.33	437275	2.57	5.35E-08
HOXA11	Homeobox A11	7p15-p14	249171	0.30	9.38E-17
KHDRBS3	KH domain, RNA binding, signal transduction associated 3	8q24.2	444558	0.48	3.46E-06
NRIP1	Nuclear receptor interacting protein 1	21q11.2	155017	0.44	2.26E-06
SHOX	Short stature homeobox	Xp22.3;Yp11.3	105932	2.26	7.35E-05
ZMIZ1	Zinc-finger, MIZ-type containing 1	10q22.3	193118	0.40	3.11E-09
<i>Signal transduction</i>					
PDE10A	Phosphodiesterase 10A	6q27	348762	0.23	5.21E-17
DDEF2	Development and differentiation enhancing factor 2	2p25 2p24	555902	0.43	1.88E-10
DUSP4	Dual specificity phosphatase 4	8p12-p11	417962	0.48	6.89E-17
FARP1	FERM, RhoGEF (ARHGEF) and pleckstrin domain protein 1	13q32.2	403917	0.43	6.83E-10
GCG	Glucagon	2q36-q37	516494	24.89	2.51E-05
GNAI1	Guanine nucleotide α inhibiting activity polypeptide 1	7q21	134587	0.33	3.40E-09
GNG12	Guanine nucleotide-binding protein (G protein), γ 12	1p31.3	696244	0.42	3.05E-06
IRS2	Insulin receptor substrate 2	13q34	442344	0.24	9.21E-20

Table 2 Continued

Gene symbol	Description	Chromosome location	UniGene ID	Fold change RT vs non-RT	P-value RT vs non-RT
PLCB1	Phospholipase C, β 1 (phosphoinositide-specific)	20p12	431173	0.33	4.87E-13
PSD3	Pleckstrin and Sec7 domain containing 3	8pter-p23.3	434255	0.45	4.76E-13
RIN2	Ras and Rab interactor 2	20p11.22	472270	0.43	1.92E-07
<i>Miscellaneous</i>					
ALDH7A1	Aldehyde dehydrogenase 7 family, member A1	5q31	483239	3.45	2.93E-04
APLP1	Amyloid β (A4) precursor-like protein 1	19q13.1	74565	2.64	1.53E-07
B4GALT5	β 1,4-galactosyltransferase, polypeptide 5	20q13.1-q13.2	370487	2.04	3.45E-04
BDH2	3-hydroxybutyrate dehydrogenase, type 2	4q24	124696	0.49	2.12E-07
BLVRB	Biliverdin reductase B	19q13.1-q13.2	515785	2.14	1.42E-06
BTBD3	BTB (POZ) domain containing 3	20p12.2	696121	0.44	5.95E-12
C12orf24	Chromosome 12 open reading frame 24	12q24.11	436618	2.24	1.50E-08
C18orf1	Chromosome 18 open reading frame 1	18p11.2	149363	0.46	6.59E-21
C1orf9	Chromosome 1 open reading frame 9	1q24	204559	2.66	1.66E-06
CHST1	Carbohydrate (keratan sulfate Gal-6) sulfotransferase 1	11p11.2-p11.1	104576	0.44	2.26E-12
CHST2	Carbohydrate (N-acetylglucosamine-6-O) sulfotransferase 2	3q24	8786	0.37	1.36E-17
COL4A2	Collagen, type IV, α 2	13q34	508716	0.26	5.75E-13
DCHS1	Dachsous 1 (Drosophila)	11p15.4	199850	0.40	6.00E-07
EMP3	Epithelial membrane protein 3	19q13.3	9999	2.14	7.03E-07
FAM59A	Family with sequence similarity 59, member A	18q12.1	444314	0.45	1.03E-07
FER1L3	Fer-1-like 3, myoferlin (<i>C. elegans</i>)	10q24	655278	4.77	5.83E-05
FLJ13197	Hypothetical FLJ13197	4p14	29725	0.34	6.73E-17
PLBD1	Putative phospholipase B-like 1 Precursor	12p13.1	131933	3.30	7.11E-10
FXYD6	FXYD domain containing ion transport regulator 6	11q23.3	635508	0.36	3.64E-07
GRB10	Growth factor receptor-bound protein 10	7p12-p11.2	164060	0.39	3.73E-13
GLUL	Glutamate-ammonia ligase	1q31	518525	0.47	1.27E-04
GYG1	Glycogenin 1	3q24-q25.1	477892	2.73	2.15E-05
KIAA0644	Unknown	7p15.1	21572	0.19	8.59E-28
LIMCH1	LIM and calponin homology domains 1	4p13	335163	0.39	1.27E-13
NIT2	Nitrilase family, member 2	3q12.2	439152	2.08	5.12E-10
PFDN4	Prefoldin subunit 4	20q13.2	91161	2.00	3.74E-05
PGAM1	Phosphoglycerate mutase 1	10q25.3	592599	2.09	5.85E-08
PLP2	Proteolipid protein 2	Xp11.23	77422	3.36	8.00E-12
PLTP	Phospholipid transfer protein	20q12-q13.1	439312	2.79	9.52E-06
PPP3CA	Protein phosphatase 3, catalytic subunit, α isoform	4q21-q24	435512	0.28	9.39E-07
SEPT11	Septin 11	4q21.1	128199	0.48	1.34E-07
SH3BP4	SH3-domain-binding protein 4	2q37.1-q37.2	516777	0.37	3.70E-10
SNX10	Sorting nexin 10	7p15.2	571296	2.16	2.72E-05
ST6GAL1	ST6 β -galactosamide α -2,6-sialyltransferase 1	3q27-q28	207459	0.43	1.24E-12
TNNT1	Troponin T type 1 (skeletal, slow)	19q13.4	631558	5.14	5.14E-07
TWF1	Twinfilin, actin-binding protein, homolog 1	12q12	189075	2.03	2.46E-04

^aAlso involved in neural development.^bAlso involved in tumor invasion/metastasis.

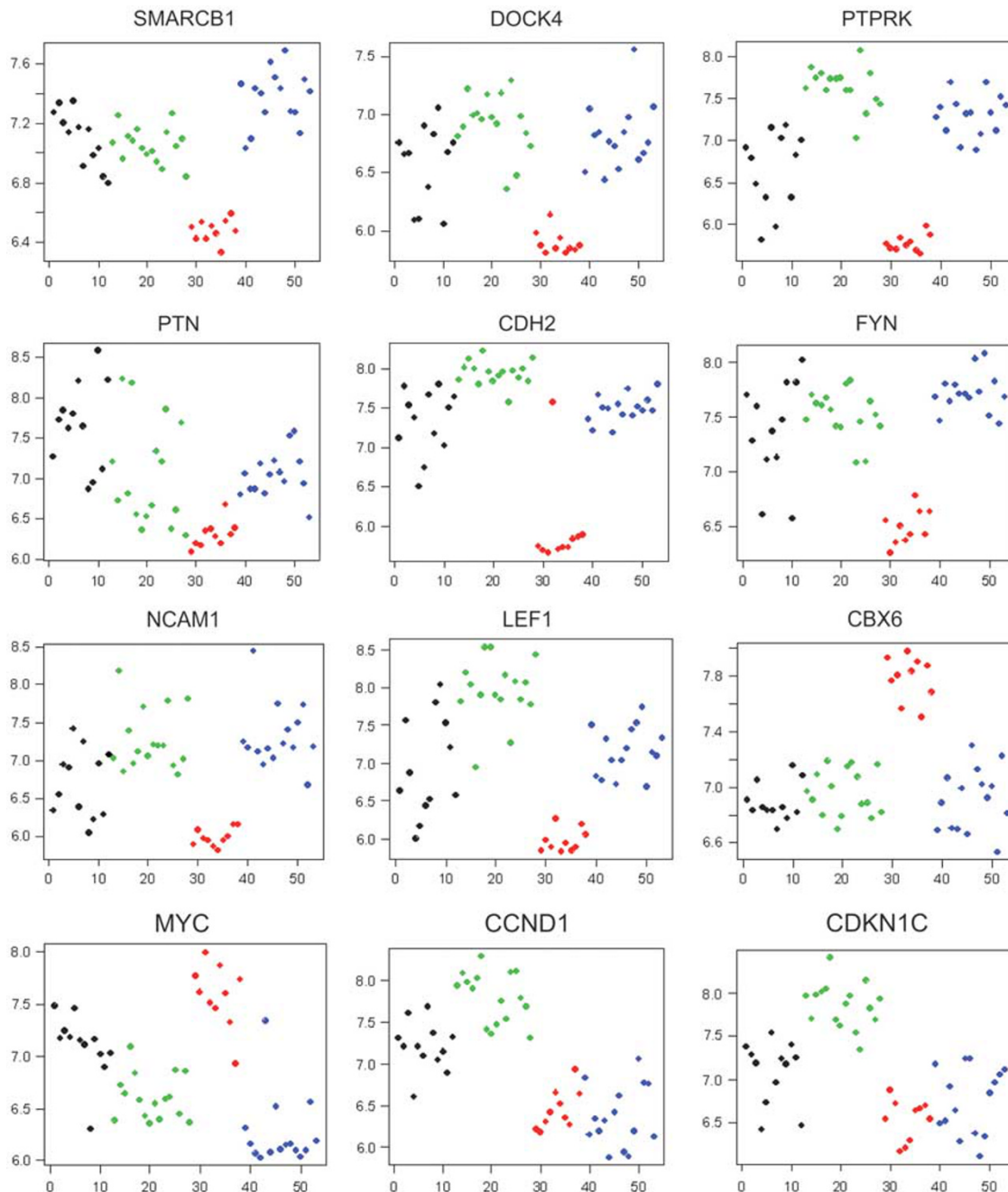


Figure 1 Patterns of gene expression within the different groups of pediatric renal tumors. The log expression levels (low to high) are plotted on the y axis. The x axis reflects an arbitrary tumor number, grouping the different tumor types starting with the congenital mesoblastic nephromas (infantile fibrosarcomas) in black, followed by clear cell sarcoma of the kidney in green, rhabdoid tumors in red, and Wilms tumors in blue.

fied in all CCSK, CMN, and WT tested. In contrast, antibodies against NQO1 showed strong positivity in all RTs and pale to no staining for the remaining tumor types (Supplementary Figure 1).

Decreased Expression of Genes Associated with Neural Development

Strikingly, 28 (25%) of the genes in Table 2 are involved with neural development and all were sharply downregulated. This

includes *SMARCB1* itself and four genes directly associated with *SMARCB1* that have previously been shown to be important in neural development (*PTN*, *DOCK4*, *SPOCK1*, and *PTPRK*). These findings are supported by analysis in PANTHER, in which the Neurogenesis group was within the top five most enriched groups of biological processes (Supplementary Table 3). To obtain more information regarding specific developmental pathways, GSEA was performed using selected groups in Gene Ontology that pertain to early

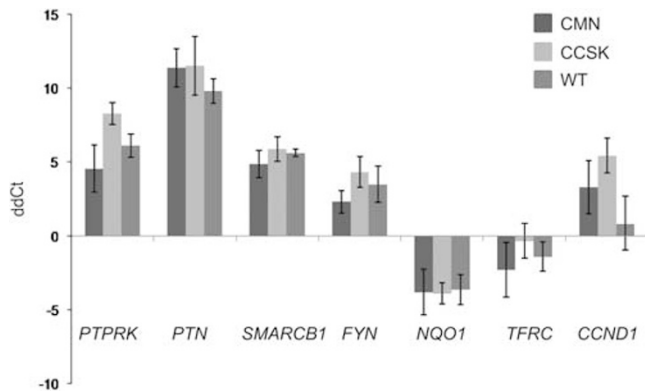


Figure 2 Validation of expression of *SMARCB1*, *FYN*, *PTN*, *NQO1*, *PTPRK*, *TFRC*, and *CCND1* using quantitative reverse transcriptase polymerase chain reaction. RNA from seven examples of each tumor type was analyzed in duplicate using the primers in Table 1. Expression changes are determined by subtracting the C_T value of the housekeeping gene (β -actin or GAPDH) from the C_T of the gene of interest (dC_T). The average dC_T from each individual tumor was subtracted from the average tumor RT dC_T value for each gene (ddC_T); these values were averaged for each tumor type and the error bars represent the standard deviation of the averages.

development pathways.¹¹ Significant enrichment was identified in non-RT compared with RT (consistent with downregulation in RT) within the following groups: GO:0022008 Neurogenesis (NES -1.59 , nominal $P=0.006$, FDR 2%), GO:0048666 Neuron Development (NES -1.53 , $P=0.008$, FDR 4%), GO:0030182 Neuron Differentiation (NES -1.48 , $P=0.008$, FDR 5%), GO:0051960 Regulation of Nervous System Development (NES -1.44 , $P=0.009$, FDR 5%). Many genes are redundant within these GO groups, therefore, a common gene list containing all genes in all the above groups was developed and is illustrated in order of rank within GSEA in Supplementary Figure 2a.

Of particular interest was the highly significant enrichment of the two available GO groups containing genes pertaining to neural crest development in non-RT (downregulation in RT). This includes GO:0014033 Neural Crest Development (NES -1.65 , $P<0.001$, FDR 2%), and GO:0001755 Neural crest migration (NES -1.60 , $P<0.001$, FDR 2%). A GSEA heatmap of all genes in both lists in rank order is illustrated in Supplementary Figure 3a. There was minimal overlap between the enriched genes of the neural development groups and those of the neural crest group. In contrast, gene sets within other early developmental GO categories (including GO:0045445 Myoblastic Differentiation, GO:0051216 Cartilage Development, GO:0001501 Skeletal development, GO:0048513 Organ development, GO:0042692 Muscle Cell Differentiation) did not show significant enrichment (defined as nominal P value <0.05 , FDR $<20\%$) in RT or non-RT. Finally, a recently published comprehensive list of genes involved in renal development was entered into GSEA and did not show significant enrichment.¹⁷ Of note, CCSKs demonstrated increased expression of genes involved with nervous system development (but not neural crest develop-

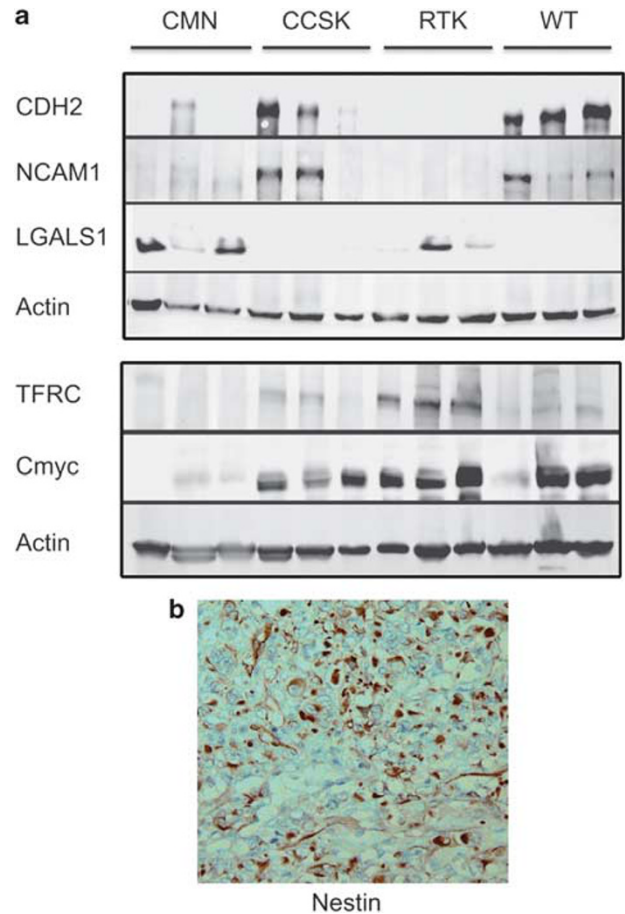


Figure 3 Protein expression in pediatric renal tumors. (a) Immunoblotting of CDH2, NCAM, LGALS1, MYC-C, and TFRC. Protein lysates from three examples of each tumor type were analyzed using antibodies provided in Table 1. Decreased expression of neural markers CDH2 and NCAM is identified in RT. Increased expression of oncogene LGALS1 is identified in 2/3 RT tested, as well as in two CMNs. Increased expression of MYC-C and one of its key targets (TFRC) is identified in RT. (b) Nestin expression in RT. Nestin mRNA was not differentially expressed in the pediatric renal tumors; however Nestin protein cytoplasmic and nuclear expression were identified in all RT tested using immunohistochemistry.

ment), as we have reported earlier.¹⁸ Therefore, all the above analyses of RT vs non-RT and fetal kidney were repeated excluding CCSKs, and all groups retained their significance (illustrated in Supplementary Figures 2b and 3b). RNA expression patterns of selected neural developmental genes from Table 2 are shown in Figure 1. Decreased expression of *FYN*, *PTN*, and *PTPRK* was verified by QRT-PCR (Figure 2). Western analysis of key neural regulators CDH2 (N-cadherin) and NCAM (CD56) proteins were entirely negative in all RT tested, with expression in 2/3 CCSKs and in all three WT tested; CMNs showed no to low expression for both markers (Figure 3a).

Several genes in Table 2 are involved in Wnt signaling (*PTN*, *DOCK4*, *CDH2*, *LEF1*, *ENCL*, *FSTL1*) or in Notch signaling (*HES1*, *NOTCH2*), and all were downregulated. Both Wnt and Notch pathways are known to be critical to

neural development. Significant negative enrichment in RT for the GO:0007219 Notch signaling pathway was identified (NES -1.48 , $P=0.02$, FDR 5%, Supplementary Figures 3c and d). However, independent gene sets available within GSEA that contain targets of Wnt signaling showed no significant enrichment of Wnt targets. When the 84 genes with human homologues on the HU133A array from the Stanford gene set of known Wnt targets was entered into GSEA and analyzed (<http://www.stanford.edu/~musse/Wntwindow.html>), there was likewise no significant enrichment in RT. Immunohistochemistry for β -catenin (*CTNNB1*) showed no nuclear staining and focal, pale cytoplasmic staining in two out of six tumors, the remaining RTs were entirely negative (data not shown).

Expression of Neural Stem Cell Markers in Rhabdoid Tumor

The striking downregulation of neural developmental markers suggests that RTs may arise within neural or neural crest stem cells followed by developmental arrest. We therefore investigated the mRNA expression of markers of known neural and neural crest stem cells, including *MSI1* (Musashi 1), *CD133* (Prominin 1), *FOXD3*, *ID3*, *SOX10*, *SNAI2*, and *SNAI1*. Of these, only *CD133* was found in Supplementary Table 1 and this was downregulated (fold change 0.3, $P=0.0002$). As these transcription factors may be regulated at very low levels, or translationally regulated, those neural crest and neural crest stem cell markers for which robust commercially available antibodies were available were analyzed, including *SOX10*, *ID3*, *Musashi*, and *CD133*. All were negative in RT with appropriate positive control staining. Of interest, antibodies directed against nestin, a marker of primitive neural as well as mesenchymal stem cells, demonstrated strong cytoplasmic positivity and scattered nuclear positivity in all RTs, with appropriate negative controls (Figure 3b). Embryonic stem cell markers *OCT4*, *NANOG*, and *SOX2* did not show differential mRNA expression or upregulation in RT.

Expression of MYC-C and its Targets

MYC-C is known to directly interact with *SMARCB1*,^{19,20} and was significantly upregulated in RT (fold change 2.37; P value 1.4×10^{-7} ; Supplementary Table 1; Figure 1). To validate the potential role for *MYC-C* upregulation in RT, the independently curated C2 gene sets within GSEA that contain *MYC-C* targets were analyzed. Significant enrichment was documented using gene sets Schumacher_MYC_UP (NES 1.56, $P=0.002$, FDR 1%) MYC_TARGETS (NES 1.44, $P=0.03$, FDR 5%), and MYC_ONCOGENIC SIGNATURES (NES 1.6, $P=0.01$, FDR 0.1%).^{21–23} A combined list containing all genes in each list was analyzed and illustrated in Supplementary Figure 4. Within Table 2, 13/114 (11%) genes are known targets of *MYC-C* and are coordinately expressed in RT (including two genes known to be downregulated by *MYC-C*). Finally, key cell-cycle genes regulated by *MYC-C*

show appropriate expression in RT, including *CCND1*, *CCND2*, *CCNE1*, *CDKN1A*, *CDKN1C*, and *CDKN2B* (see below). Confirmation of expression of *MYC-C* and *TFRC* (a *MYC-C* target) proteins was performed and illustrated in Figure 3a; confirmation of mRNA expression of *TFRC* using QRT-PCR was also performed (Figure 2).

Cell-Cycle Gene Expression

Numerous studies have shown that re-expression of *SMARCB1* in RT-derived cell lines results in upregulation of *CDKN1A* (p21CIP/WAF1) and *CDKN2A* (p16INK4a) and downregulation of *CCND1* (cyclin D1), *CCNE1* (cyclin E), *CCNA1* (cyclin A), with secondary phosphorylated RB protein, cellular senescence, and apoptosis.^{24–26} Most of these findings are confirmed in the human RTs analyzed in our study, with some exceptions. Of the cyclin-dependent kinase inhibitors, both *CDKN1A* and *CDKN2A* are expressed at very low levels in all renal tumor types tested, including RT. *CDKN1C* (p57kip2) mRNA was also significantly downregulated in RT (fold change 0.4; $P=2.15 \times 10^{-6}$) (Supplementary Table 1; Figure 1). Immunohistochemistry for *CDKN1A* and *CDKN1B* showed staining of fewer than 1% of tumor cells in all renal tumors tested (data not shown). Of the cyclin-dependent kinases, *CCND2* and *CCNE* mRNAs were not differentially expressed but were upregulated in all tumors, and antibodies to both cyclin E and cyclin D2 confirmed strong nuclear staining within the majority of RT cells (data not shown). Immunostaining for p53 was positive in fewer than 1% of RT nuclei. In contrast with prior studies, *CCND1* mRNA was downregulated in RT in our study (FC 0.4, $P=1.2 \times 10^{-5}$, Figure 1). This was confirmed by quantitative RT-PCR (Figure 2) and immunohistochemistry showed protein expression in fewer than 1% of RT cells in the face of strong nuclear positivity in CCSKs, WT, and CMN (Supplementary Figure 1). (Of note, cyclin D2 and cyclin E are activated by *CMYC*,²⁷ whereas *CMYC* has been shown to repress *CCND1*,²⁸ *CDKN1A*, and *CDKN2B*.²¹)

Differential Expression of Genes Associated with Tumor Suppression, Invasion, and Metastasis

Many of the top 114 genes in Table 2 are recognized oncogenes yet were downregulated in RT. Conversely, 10 genes associated with tumor suppression, invasion, or metastasis demonstrated regulation in RT concordant with their activity and therefore represent potential therapeutic targets. *SPP1* (osteopontin), *MMP12*, *NCOA3*, *TFRC*, *RSU1*, and *ZNF217* are associated with tumor invasion and metastasis and were upregulated; *SELENBP*, *COL18A1* (endostatin), *PTPRK*, and *DOCK4* have tumor suppression functions and were downregulated (Table 2; Figures 1 and 4). Of these, *PTPRK* and *DOCK4* have been previously directly associated with *SMARCB1* expression.^{12,13} Additional potential therapeutic targets found in Supplementary Table 1 include *LGALS1* (fold change 1.7, $P=1.07 \times 10^{-5}$) and *SERPINF1* (pigmented epithelium-derived factor (PEDF)) (fold change 2.3,

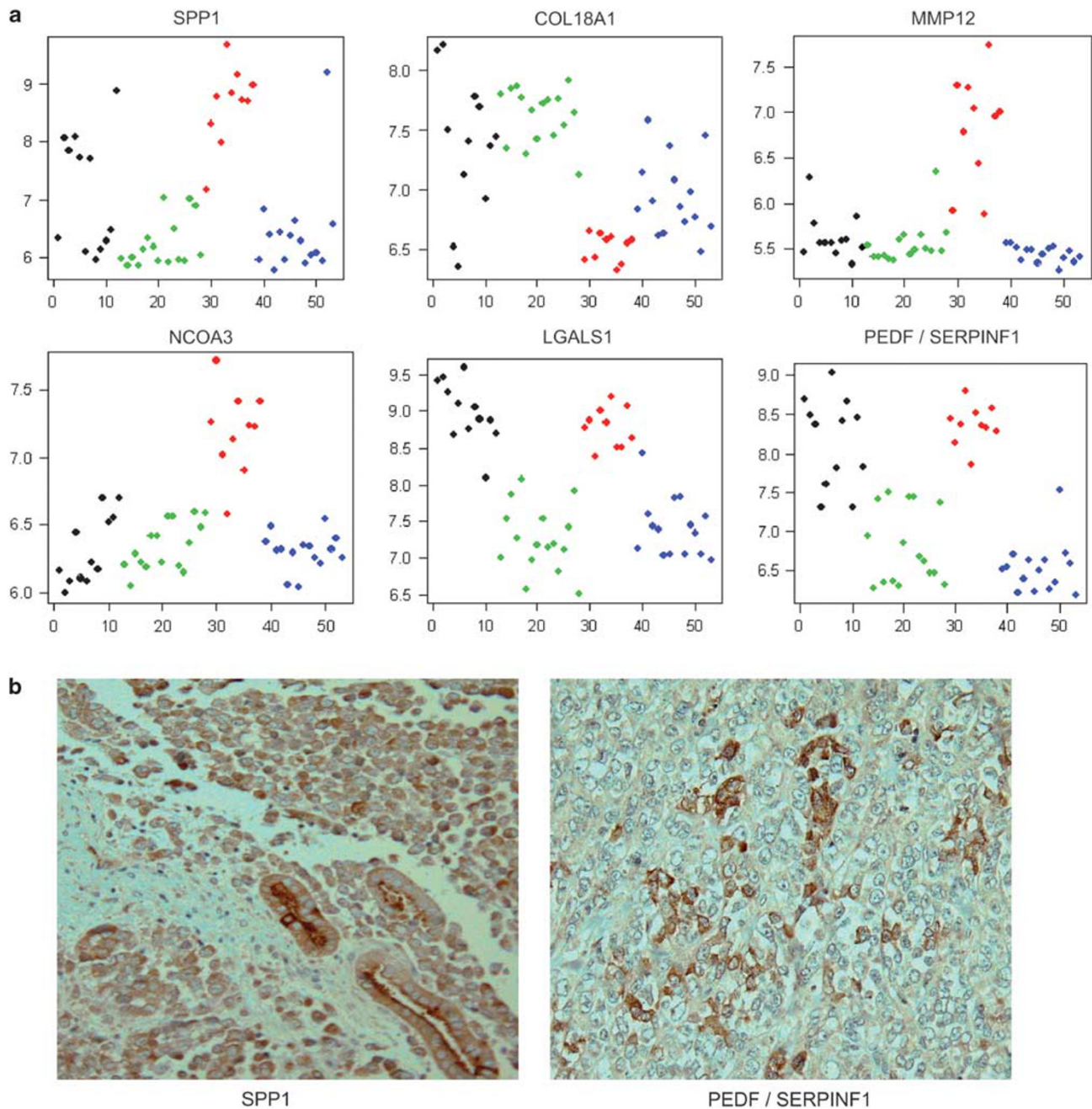


Figure 4 Expression of selected genes involved in tumor invasion and metastasis. **(a)** Pattern of RNA expression of key genes. The expression levels (low to high) are plotted on the y axis. The x axis groups the different tumor types starting with the congenital mesoblastic nephromas (infantile fibrosarcomas) in black, followed by clear cell sarcoma of the kidney in green, rhabdoid tumors in red, and Wilms tumors in blue. **(b)** Protein expression of SPP1 and PEDF (SERPINF1). The majority of cells within all RT show moderate positivity for SPP1. Note the striking positivity of non-neoplastic renal tubules for SPP1. Clusters of cells within RT show strong positivity for PEDF.

$P = 3.4 \times 10^{-11}$). These were not included in the top gene list because of their high expression in CMN as well as RT (Figure 4). Both *LGALS1* and *SPP1* were significantly upregulated in previous gene expression analysis studies.^{15,16} Differential expression of *TFRC* and *PTPRK* were validated by QRT-PCR (Figure 2). Expression of SPP1 (osteopontin), PEDF, and TFRC proteins in RT was demonstrated by immunohistochemistry or immunoblotting (Figures 3 and 4).

Expression of Genes Associated with Transcription Regulation

In addition to MYC-C, a number of genes involved in transcription regulation and signal transduction were upregulated in RT. Of particular note, *CBX6* was highly upregulated (Figure 1; Table 2). *CBX6* is a member of the polycomb family, which is responsible for transcriptional repression mediated by the specific H3K27 histone methylation. Our

data show loss of expression of *GRB10* and *CDKN1C* in RT, both of which are epigenetically regulated by the specific H3K27 trimethylation mediated by the polycomb group.^{29,30} RTs also showed loss of expression of multiple HOX genes, long known to be repressed by polycomb group proteins.³¹ (In Supplementary Table 1, *HOXA10*, *HOXA11*, *HOXC4*, *HOXD3*, *HOXD4*, *HOXD9*, *HOXD10*, *HOXD11* are all downregulated.) In contrast to the polycomb group, the trithorax family is responsible for transcriptional activation mediated by the specific H3K4 methylation. *MLL1*, the predominant member of the trithorax family in humans, is known to achieve transcriptional activation by interacting directly with SMARCB1.³² Of further interest in this regard is the newly described role of *ZNF217* as an organizer of repressive histones. *ZNF217* (an oncogene significantly upregulated in RT, Table 2) has been shown to demethylate H3K4me3 and to methylate H3K27 through interaction with EZH2, a member of the polycomb repressive complex 2.³³ Therefore, the transcriptional repression seen in RT may be associated with histone 3 modifications.

To investigate this hypothesis, we relied on the availability of whole genomic surveys of methylation markers within embryonic stem cells (ESC). Zhao *et al*³⁴ classified the H3K4me3 and H3K27me3 markers associated with over 17000 genes in ESC and established three groups of genes: Group 1 with neither H3K4 nor H3K27me3 modification, Group 2 with only H3K4me3 modification, and Group 3 with both H3K4 and H3K27me3 (bivalent). We placed the gene list from each group in GSEA to determine whether their expression was enriched in RT or non-RT. The expression of genes in Groups 1 and 2 did not show significant enrichment in either RT or non-RT. However, the 1141 genes in Group 3 (those bivalently modified in ESC) showed significant enrichment in non-RT, indicating decreased expression in RT (NES -1.5 , $P = 0.01$, FDR 5%, Supplementary Figure 5a). When the other pediatric renal tumors were similarly analyzed (leaving RT out), no significant enrichment was identified in either CMN or WT. In contrast, CCSK showed significant positive enrichment for Group 3 genes. Therefore, we again analyzed Group 3 genes comparing RT to non-RT leaving out the CCSKs, and significant enrichment non-RT was retained ($P < 0.001$, Supplementary Figure 5b). Of note, 11% of genes in Supplementary Table 1 are Group 3 genes, and 90% of these genes show decreased expression in RT. Zhao *et al*³⁴ also demonstrated the top GO categories differentially represented through PANTHER in Group 3 to be genes important for developmental processes, ectoderm development, neurogenesis, transcription regulation, and signal transduction. Within RT, with the exception of transcription regulation, using PANTHER we found the same top categories at the top of our list (Supplementary Table 3). Finally, we performed a similar *in silico* analysis of 512 targets of Polycomb Repressive Complex 2 in ESC.³⁵ GSEA analysis again revealed significant enrichment in non-RT (NES -1.4 , $P = 0.05$, FDR 9%).

DISCUSSION

RT are rare tumors that are virtually confined to infancy and are characterized by loss of the *SMARCB1/hSNF5/INI-1* gene.^{4,36} SMARCB1 is one of over 10 non-catalytic subunits of the highly evolutionarily conserved SWI/SNF ATP-dependent chromatin-remodeling complex expressed in all normal cells at all stages of development.⁶ SMARCB1 is recognized as a tumor suppressor gene because of its biallelic involvement in the development of RT, reviewed by Biegel *et al*.³⁶ The SWI-SNF complex appears to relieve repressive chromatin structures by disrupting the DNA-histone interaction within nucleosomes, allowing the transcriptional machinery to access its targets more effectively, facilitating transcriptional activation and repression (previously reviewed by Stojanova and Penn³⁷ and Roberts and Orkin³⁸). The current hypothesis is that SMARCB1, through its ability to bind to several proteins, serves to recruit the SWI/SNF complex to specific target sites thereby mediating transcription regulation.^{38,39} However, precisely how SMARCB1 accomplishes this is largely unknown. Proteins that have been demonstrated by others to physically interact with SMARCB1 or to be direct targets of SMARCB1 include MLL, MYC-C, PTN, HESR1, ATP1B1, and FZD7.^{12,20,32} Our gene expression analysis demonstrates key roles for these genes and others in the development of human RT, as discussed below.

SMARCB1 Loss Results in Repression of Genes Critical to Neural and Neural Crest Development

Genes involved with neural and neural crest development were sharply downregulated in RT. A number of recent studies have shown that SWI/SNF itself is required for normal vertebrate neurogenesis.^{40,41} Pleiotrophin, *PTN*, has been shown to directly interact with SMARCB1¹² and to regulate the balance between differentiation and proliferation within neural stem cells by inhibiting proliferation and enhancing differentiation.⁴² The Notch signaling pathway is also critical for controlling the induction of neural development and for maintaining the neural progenitor population.⁴³ Within the Notch pathway, HESR1 (*HEY1*) is a known direct target of SMARCB1,¹² and recruitment of SMARCB1 to the HES1 and HES5 promoters has been demonstrated. *NOTCH2* and *HES1* (the ligand of HESR1) were both downregulated in RT (Table 2) and GSEA analysis confirmed the downregulation of the Notch signaling pathway in RT. Finally, a large number of important downstream transcription factors involved with neural and neural crest development were likewise sharply downregulated, including *NCAM* (regulated by HES1), *CDH2* (neural-cadherin), *FYN* (a downstream target of *PTN*), and *SOX11*, which induces differentiation within neural stem cells and regulates various aspects of neural crest development.⁴⁴ In summary, RTs show striking repression of neural differentiation, suggesting the possibility that RTs may arise in progenitor cells in which *SMARCB1* loss results in prevention of neural development. This is supported by neural differentiation that develops within cell lines derived

from both CNS and extra-CNS soft tissue RTs when *SMARCB1* is re-introduced.⁴⁵

Neural development begins within the embryonic ectoderm from which the neural plate differentiates. The neural plate folds to form the neural tube which then differentiates into the structures of the central nervous system. Cells of the neural crest arise at the border between the neural plate and the ectoderm for the entire length of the neuraxis (previously reviewed by Barembaum and Bronner-Fraser⁴⁶). After induction, the neural crest cells migrate as undifferentiated precursor cells to various parts of the embryo where they differentiate into many cell types including cells of sensory neurons and glia of the peripheral nervous system, bone, cartilage, and melanocytes. Therefore, the ability to show divergent differentiation, the ability to migrate over considerable distances, and presence in both CNS and extra-CNS sites are features shared by both neural crest stem cells and RTs. Our study reveals significant downregulation of both neural and neural crest developmental genes. To address the hypothesis that RT develop within neural or neural crest stem cells with arrested development, we investigated the mRNA and protein expression of key neural and neural crest stem cell markers.^{46–50} Low to no expression of early neural and neural crest stem cell markers *SNAIL1*, *SLUG*, *FOXD3*, *SOX10*, *ID3*, *CD133*, *Musashi* was identified. Embryonic stem cell markers *OCT4*, *NANOG*, *SOX2* were also not upregulated in RT. In contrast, strong expression of nestin was identified in RT. Nestin has been shown to be abundantly expressed in embryonic stem cell-derived progenitor cells that have the potential to develop into neuroectodermal, endodermal, and mesodermal lineages.⁵¹ Our data therefore suggest that RTs do not arise in neural or neural crest stem cells *per se*, but instead may arise in early progenitor cells after the differentiation trigger (and after loss of ESC markers) in cells destined to become neural and/or neural crest stem cells. Loss of *SMARCB1* at this critical period of time may suppress neural and/or neural crest stem cell development.

Transcriptional Repression may Play a Role in RT Development

Clues toward the mechanisms involved in this developmental repression are provided by evidence that *SMARCB1* loss may result in alterations in the activity of the trithorax and polycomb families, which are responsible for maintaining the reciprocal transcriptional states of key developmental regulators.⁵² MLL1, the key member of the trithorax group in humans, is a ubiquitously expressed nuclear protein that has been shown to interact directly with *SMARCB1* through the MLL *SET* domain, resulting in remodeling of chromatin and transcriptional activation.⁵² MLL1 mediates transcriptional activation by catalyzing the methylation of histone H3 lysine 4 (H3K4me).⁵³ MLL1 has also been shown to be required for neurogenesis.⁵⁴ In contrast, the polycomb group (Pcg) mediates transcriptional repression through catalyzing the

methylation of histone H3 lysine 27 (H3K27me).³¹ These critical histone 3 modifications have been comprehensively mapped across the genome in both human and mouse embryonic stem cells using varied experimental approaches.^{34,55,56} These studies, which show striking concordance, show that the majority of genes in ESC are marked with H3K4 alone (50–58%) or in combination with H3K27 (bivalent, 10–17%), whereas 28–33% show neither marking. The majority of genes with H3K4 methylation alone are associated with basic cellular functions such as housekeeping genes, proliferation, protein, and DNA metabolism, etc. In contrast, genes bivalently modified were enriched in GO developmental functions, particularly those involving neurogenesis, ectoderm differentiation, transcriptional regulation, and signal transduction. These bivalently marked genes overlapped considerably with genes demonstrated to be polycomb group targets.³⁵ Indeed, bivalent genes appear to be dominated by the H3K27 repressive markers and to be downregulated in ESC. The presence of the H3K4 methylation in these bivalently modified histones may serve to enable a sharp increase in expression of lineage-specific transcription markers after the trigger for differentiation.^{34,35,55,56}

Our study shows that the same developmental pathways and genes that are marked by bivalently modified histones and downregulated within ESC are likewise significantly downregulated in RT. These include the processes of neurogenesis, signal transduction, and ectoderm differentiation (Supplementary Table 3). Further, genes bivalently modified in ESC were among those that most strongly differentiated RT from non-RT by GSEA (Supplementary Figure 5). Analyses of independent sets of genes known to be polycomb targets³⁵ likewise demonstrated the same findings. These analyses suggest that RT may arise within early stem cells whose bivalently modified histones remain dominated by the polycomb group histone markings. At the time of differentiation, this repression would generally be overcome by SWI/SNF, but in the absence of *SMARCB1* this does not occur. Indeed, there is growing evidence that SWI/SNF may have an integral role in the balance between trithorax and polycomb group activity through the direct interaction between *SMARCB1* and MLL1. This is best seen in a series of experiments that focused on the colocalized p16/INK4a and p14/ARF tumor suppressor genes. P16 is known to be repressed because of polycomb group-mediated H3K27 methylation, whereas the nearby p14 is not.⁵⁷ Re-expression of *SMARCB1* within RT cell lines has been shown to result in induction of p16 but not p14.^{24,58} Kia *et al*⁵⁹ performed chromatin immunoprecipitation demonstrating that *SMARCB1* bound strongly to the p16 promoter, but not to the p14 promoter. Further, in the absence of *SMARCB1*, polycomb group silencers (PRC1, PRC2) were present in large amounts on the p16 promoter, but in low amounts on the p14 promoter. Re-expression of *SMARCB1* resulted in the following: (1) reduced binding of PRC1 and PRC2 and increased MLL1 binding at the p16 promoter; (2) reduced

H3K27 and increased H3K4 methylation at the p16 promoter; and (3) activated p16. On the basis of these *CDKN2A* studies, Kia *et al* concluded that polycomb group silencers are evicted by SWI/SNF, thereby allowing for chromatin modification. In the absence of *SMARCB1*, this did not occur. Our data suggest that this mechanism may occur more widely within bivalently modified genes in development. Indeed, a broader role of the SWI/SNF chromatin remodeling complex in development is suggested by studies showing that *SMARCB1* is required for hepatocyte and adipocyte development.^{60,61}

It should be noted that there are a number of different histone modifications in addition to H3 methylation, which impact on gene expression. Furthermore, many histone modifications interact with one another, creating extreme complexity. To add to this potential complexity within RT is the presence of MYC-C activation. MYC-C is a transcription factor, which has long been known to drive a large number of diverse biological activities during development and oncogenesis. In recent years, it has become apparent that MYC-C may modulate transcription, in part at least, through H3 and H4 acetylation.⁶² A physical interaction between *SMARCB1* and MYC-C proteins has been documented by several laboratories and the SNF complex acts directly to repress MYC-C during differentiation.^{19,20,27,63} Finally, MYC-C has been shown to be critical regulator of neural crest formation.⁶⁴ It is clear that further investigation is needed to clarify the interface between the two broad processes involved in chromatin remodeling, namely histone modification and the ATP-dependent nucleosomal remodeling mediated by SWI/SNF.

RT Show Decreased Cyclin-Dependent Kinase Inhibition

Numerous publications have implicated multiple members of the SWI/SNF complex in cell-cycle control. Several laboratories have demonstrated downregulation of cyclin-dependent kinase inhibitors *CDKN1A* and/or *CDKN2A* (*p16/INK4a*), and their upregulation on reintroduction of *SMARCB1*, accompanied by growth arrest.^{24,26,59} Mutation analysis of these genes in RT is not available in the literature. These observations would predict upregulation of *MYC*, downregulation of both *CDKN1A* and *CDKN2A*, and upregulation of cyclins A and E within RT, all of which are confirmed in our study. We also show downregulation of *CDKN1C* (p57Kip2), a major regulator of embryonic growth, that has recently been shown to be a downstream target of *SMARCB1*.⁶⁵ Of interest, both *CDKN1C* and *CDKN2A* are regulated in part through the polycomb group by methylation of H3K27.³⁰ Therefore, our data support that of other studies that indicate a proliferative advantage of RT through loss of cyclin-dependent kinase inhibition directly linked to *SMARCB1* loss.

Several previous studies based primarily on RT cell lines have suggested that cyclin D1 is a direct target of *SMARCB1* and may be a possible therapeutic target.^{25,66,67} It was

therefore surprising that neither our data nor gene expression after *SMARCB1* induction in RT-derived cell lines¹² supports these findings. Instead, our study shows decreased expression of *CCND1* at both the RNA and protein levels. A likely mechanism for downregulation of *CCND1* in RT is upregulation of *MYC-C*, which is known to repress *CCND1* expression at its promoter.²⁸

Potential Therapeutic Targets

RTs are highly malignant and lethal tumors, and the ultimate goal of this study is to improve their clinical outcome. Analysis of gene expression shows differential expression of a number of genes known to cause tumor suppression or tumor progression. In particular, two putative tumor suppressor genes have been shown earlier to be directly associated with *SMARCB1* and are downregulated in RTs, *PTPRK*, and *DOCK4*. *PTPRK* (protein-tyrosine phosphatase receptor- κ) dephosphorylates EGFR, the prototypic receptor protein tyrosine kinase, and thereby regulates growth and survival.⁶⁸ *DOCK4* promotes β -catenin stability and is disrupted during tumorigenesis through mutation and deletion in several human cancers.^{69,70} In addition, two known therapeutic targets differentially expressed in RT include *SPP1* and *COL18A1*. *SPP1* (osteopontin) is a secreted phosphoprotein involved in immunity, angiogenesis, cell migration, and cell survival. Overexpression of *SPP1* is associated with aggressiveness and metastasis in many different tumor types and is an independent predictor of behavior in melanomas, a tumor derived from the neural crest.⁷¹ Inhibition of *SPP1* expression can reverse this phenotype.⁷² Previous reports have demonstrated elevated *SPP1* plasma levels and expression levels in RT.⁷³ *SPP1* is cleaved into biologically active fragments by *MMP12*.⁷⁴ Our study shows both *SPP1* and *MMP12* to be upregulated in RT. C-terminal cleavage of *COL18A1* (downregulated in RT) results in the protein endostatin, a potent endogenous inhibitor of angiogenesis, migration, and invasion (previously reviewed by Abdollahi *et al*⁷⁵). In clinical trials, recombinant endostatin inhibited the growth of a variety of tumors while exhibiting no apparent toxic side effects.⁷⁶

Other genes involved in tumorigenesis or tumor progression were differentially expressed in RT. *PEDF* (or *SERPINF1*) has neuroprotective and antiangiogenic effects, suppresses cell-cycle progression, and supports neural stem cell self-renewal.⁷⁷ Notably, *PEDF* protein is broadly expressed in the nervous system and circulates in plasma and cerebrospinal fluid and therefore may be useful as a diagnostic marker. *LGALS1* (upregulated in RT in both our study as well as that of Pomeroy *et al*¹⁵) also has a well-documented role in tumorigenesis, metastasis, and invasion.⁷⁸

Conclusions

The data presented suggest that RT arise within an early progenitor population during a critical developmental window. In these cells, loss of *SMARCB1* results in (1) repression

of neural development, (2) transcriptional repression that may be mediated by dysregulation of, or loss of interaction with, the trithorax/polycomb groups, (3) silencing of cyclin-dependent kinase inhibitors, and (4) differential expression of a number of prominent genes that are known to promote malignant behavior and represent potential therapeutic targets.

Supplementary Information accompanies the paper on the Laboratory Investigation website (<http://www.laboratoryinvestigation.org>)

ACKNOWLEDGEMENT

We acknowledge the expertise of Donna Kersey, Patricia Beezhold, and Debra Haftl, who contributed greatly to this effort. Work supported by NIH U01 CA114757 (EJP, CCH), and NIH U10 CA98543 (EJP).

DISCLOSURE/CONFLICT OF INTEREST

The authors declare no conflict of interest.

- Tomlinson GE, Breslow NE, Dome J, *et al*. Rhabdoid tumor of the kidney in the National Wilms Tumor Study: age at diagnosis as a prognostic factor. *J Clin Oncol* 2005;23:7641–7645.
- Rorke LB, Packer R, Biegel J. Central nervous system atypical teratoid/rhabdoid tumors of infancy and childhood. *J Neurooncol* 1995;24:21–28.
- Burger PC, Yu IT, Tihan T, *et al*. Atypical teratoid/rhabdoid tumor of the central nervous system: a highly malignant tumor of infancy and childhood frequently mistaken for medulloblastoma: a Pediatric Oncology Group study. *Am J Surg Pathol* 1998;22:1083–1092.
- Versteeg I, Sevenet N, Lange J, *et al*. Truncating mutations of hSNF5/INI1 in aggressive pediatric cancer. *Nature* 1998;394:203–206.
- Biegel JA, Tan L, Zhang F, *et al*. Alterations of the hSNF5/INI1 gene in central nervous system atypical teratoid/rhabdoid tumors and renal and extrarenal rhabdoid tumors. *Clin Cancer Res* 2002;8:3461–3467.
- Imbalzano AN, Jones SN. Snf5 tumor suppressor couples chromatin remodeling, checkpoint control, and chromosomal stability. *Cancer Cell* 2005;7:294–295.
- Huang CC, Cutcliffe C, Coffin C, *et al*. Classification of malignant pediatric renal tumors by gene expression. *Pediatr Blood Cancer* 2006;46:728–738.
- Hoot AC, Russo P, Judkins AR, *et al*. Immunohistochemical analysis of hSNF5/INI1 distinguishes renal and extra-renal malignant rhabdoid tumors from other pediatric soft tissue tumors. *Am J Surg Pathol* 2004;28:1485–1491.
- Argani P, Fritsch M, Kadkol SS, *et al*. Detection of the ETV6-NTRK3 chimeric RNA of infantile fibrosarcoma/cellular congenital mesoblastic nephroma in paraffin-embedded tissue: application to challenging pediatric renal stromal tumors. *Mod Pathol* 2000;13:29–36.
- Thomas PD, Campbell MJ, Kejariwal A, *et al*. PANTHER: a library of protein families and subfamilies indexed by function. *Genome Res* 2003;13:2129–2141.
- Subramanian A, Tamayo P, Mootha VK, *et al*. Gene set enrichment analysis: a knowledge-based approach for interpreting genome-wide expression profiles. *Proc Natl Acad Sci USA* 2005;102:15545–15550.
- Medjkane S, Novikov E, Versteeg I, *et al*. The tumor suppressor hSNF5/INI1 modulates cell growth and actin cytoskeleton organization. *Cancer Res* 2004;64:3406–3413.
- Isakoff MS, Sansam CG, Tamayo P, *et al*. Inactivation of the Snf5 tumor suppressor stimulates cell cycle progression and cooperates with p53 loss in oncogenic transformation. *Proc Natl Acad Sci USA* 2005;102:17745–17750.
- Morozov A, Lee SJ, Zhang ZK, *et al*. INI1 induces interferon signaling and spindle checkpoint in rhabdoid tumors. *Clin Cancer Res* 2007;13:4721–4730.
- Pomeroy SL, Tamayo P, Gaasenbeek M, *et al*. Prediction of central nervous system embryonal tumour outcome based on gene expression. *Nature* 2002;415:436–442.
- Ma HI, Kao CL, Lee YY, *et al*. Differential expression profiling between atypical teratoid/rhabdoid and medulloblastoma tumor *in vitro* and *in vivo* using microarray analysis. *Childs Nerv Syst* 2009;26:293–303.
- Brunskill EW, Aronow BJ, Georgas K, *et al*. Atlas of gene expression in the developing kidney at microanatomic resolution. *Dev Cell* 2008;15:781–791.
- Cutcliffe C, Kersey D, Huang CC, *et al*. Clear cell sarcoma of the kidney: upregulation of neural markers with activation of the sonic hedgehog and Akt pathways. *Clin Cancer Res* 2005;11:7986–7994.
- Nagl Jr NG, Zweitig DR, Thimmapaya B, *et al*. The c-myc gene is a direct target of mammalian SWI/SNF-related complexes during differentiation-associated cell cycle arrest. *Cancer Res* 2006;66:1289–1293.
- Cheng SW, Davies KP, Yung E, *et al*. c-MYC interacts with INI1/hSNF5 and requires the SWI/SNF complex for transactivation function. *Nat Genet* 1999;22:102–105.
- Zeller KI, Jegga AG, Aronow BJ, *et al*. An integrated database of genes responsive to the Myc oncogenic transcription factor: identification of direct genomic targets. *Genome Biol* 2003;4:R69.
- Schuhmacher M, Kohlhuber F, Holzel M, *et al*. The transcriptional program of a human B cell line in response to Myc. *Nucleic Acids Res* 2001;29:397–406.
- Bild AH, Yao G, Chang JT, *et al*. Oncogenic pathway signatures in human cancers as a guide to targeted therapies. *Nature* 2006;439:353–357.
- Betz BL, Strobeck MW, Reisman DN, *et al*. Re-expression of hSNF5/INI1/BAF47 in pediatric tumor cells leads to G1 arrest associated with induction of p16ink4a and activation of RB. *Oncogene* 2002;21:5193–5203.
- Zhang ZK, Davies KP, Allen J, *et al*. Cell cycle arrest and repression of cyclin D1 transcription by INI1/hSNF5. *Mol Cell Biol* 2002;22:5975–5988.
- Chai J, Charboneau AL, Betz BL, *et al*. Loss of the hSNF5 gene concomitantly inactivates p21CIP/WAF1 and p16INK4a activity associated with replicative senescence in A204 rhabdoid tumor cells. *Cancer Res* 2005;65:10192–10198.
- Amati B, Frank SR, Donjerkovic D, *et al*. Function of the c-Myc oncoprotein in chromatin remodeling and transcription. *Biochim Biophys Acta* 2001;1471:M135–M145.
- Philipp A, Schneider A, Vasrik I, *et al*. Repression of cyclin D1: a novel function of MYC. *Mol Cell Biol* 1994;14:4032–4043.
- Yamasaki-Ishizaki Y, Kayashima T, Mapendano CK, *et al*. Role of DNA methylation and histone H3 lysine 27 methylation in tissue-specific imprinting of mouse Grb10. *Mol Cell Biol* 2007;27:732–742.
- Umlauf D, Goto Y, Cao R, *et al*. Imprinting along the Kcnq1 domain on mouse chromosome 7 involves repressive histone methylation and recruitment of Polycomb group complexes. *Nat Genet* 2004;36:1296–1300.
- Cao R, Wang L, Wang H, *et al*. Role of histone H3 lysine 27 methylation in Polycomb-group silencing. *Science* 2002;298:1039–1043.
- Rozenblatt-Rosen O, Rozovskaia T, Burakov D, *et al*. The C-terminal SET domains of ALL-1 and TRITHORAX interact with the INI1 and SNR1 proteins, components of the SWI/SNF complex. *Proc Natl Acad Sci USA* 1998;95:4152–4157.
- Banck MS, Li S, Nishio H, *et al*. The ZNF217 oncogene is a candidate organizer of repressive histone modifiers. *Epigenetics* 2009;4:100–106.
- Zhao XD, Han X, Chew JL, *et al*. Whole-genome mapping of histone H3 Lys4 and 27 trimethylations reveals distinct genomic compartments in human embryonic stem cells. *Cell Stem Cell* 2007;1:286–298.
- Boyer LA, Plath K, Zeitlinger J, *et al*. Polycomb complexes repress developmental regulators in murine embryonic stem cells. *Nature* 2006;441:349–353.
- Biegel JA, Kalpana G, Knudsen ES, *et al*. The role of INI1 and the SWI/SNF complex in the development of rhabdoid tumors: meeting summary from the workshop on childhood atypical teratoid/rhabdoid tumors. *Cancer Res* 2002;62:323–328.
- Stojanova A, Penn LZ. The role of INI1/hSNF5 in gene regulation and cancer. *Biochem Cell Biol* 2009;87:163–177.
- Roberts CW, Orkin SH. The SWI/SNF complex—chromatin and cancer. *Nat Rev Cancer* 2004;4:133–142.

39. Martens JA, Winston F. Recent advances in understanding chromatin remodeling by Swi/Snf complexes. *Curr Opin Genet Dev* 2003;13:136–142.
40. Seo S, Richardson GA, Kroll KL. The SWI/SNF chromatin remodeling protein Brg1 is required for vertebrate neurogenesis and mediates transactivation of *Ngn* and *NeuroD*. *Development* 2005;132:105–115.
41. Aigner S, Denli AM, Gage FH. A novel model for an older remodeler: the BAF swap in neurogenesis. *Neuron* 2007;55:171–173.
42. Hienola A, Pekkanen M, Raulo E, *et al*. HB-GAM inhibits proliferation and enhances differentiation of neural stem cells. *Mol Cell Neurosci* 2004;26:75–88.
43. Sakamoto M, Hirata H, Ohtsuka T, *et al*. The basic helix-loop-helix genes *Hes1/Hey1* and *Hes2/Hey2* regulate maintenance of neural precursor cells in the brain. *J Biol Chem* 2003;278:44808–44815.
44. Hong CS, Saint-Jeannet JP. Sox proteins and neural crest development. *Semin Cell Dev Biol* 2005;16:694–703.
45. Albanese P, Belin MF, Delattre O. The tumour suppressor *hSNF5/INI1* controls the differentiation potential of malignant rhabdoid cells. *Eur J Cancer* 2006;42:2326–2334.
46. Barembaum M, Bronner-Fraser M. Early steps in neural crest specification. *Semin Cell Dev Biol* 2005;16:642–646.
47. Kim J, Lo L, Dormand E, *et al*. *SOX10* maintains multipotency and inhibits neuronal differentiation of neural crest stem cells. *Neuron* 2003;38:17–31.
48. Aybar MJ, Nieto MA, Mayor R. Snail precedes slug in the genetic cascade required for the specification and migration of the *Xenopus* neural crest. *Development* 2003;130:483–494.
49. Light W, Vernon AE, Lasorella A, *et al*. *Xenopus* *Id3* is required downstream of *Myc* for the formation of multipotent neural crest progenitor cells. *Development* 2005;132:1831–1841.
50. Corti S, Nizzardo M, Nardini M, *et al*. Isolation and characterization of murine neural stem/progenitor cells based on *Prominin-1* expression. *Exp Neurol* 2007;205:547–562.
51. Wiese C, Rolletschek A, Kania G, *et al*. Nestin expression—a property of multi-lineage progenitor cells? *Cell Mol Life Sci* 2004;61:2510–2522.
52. Terranova R, Agherbi H, Boned A, *et al*. Histone and DNA methylation defects at *Hox* genes in mice expressing a SET domain-truncated form of *Mll*. *Proc Natl Acad Sci USA* 2006;103:6629–6634.
53. Milne TA, Briggs SD, Brock HW, *et al*. *MLL* targets SET domain methyltransferase activity to *Hox* gene promoters. *Mol Cell* 2002;10:1107–1117.
54. Lim DA, Huang YC, Swigut T, *et al*. Chromatin remodelling factor *Mll1* is essential for neurogenesis from postnatal neural stem cells. *Nature* 2009;458:529–533.
55. Pan G, Tian S, Nie J, *et al*. Whole-genome analysis of histone H3 lysine 4 and lysine 27 methylation in human embryonic stem cells. *Cell Stem Cell* 2007;1:299–312.
56. Mikkelsen TS, Ku M, Jaffe DB, *et al*. Genome-wide maps of chromatin state in pluripotent and lineage-committed cells. *Nature* 2007;448:553–560.
57. Sparmann A, van Lohuizen M. Polycomb silencers control cell fate, development and cancer. *Nat Rev Cancer* 2006;6:846–856.
58. Oruetebarria I, Venturini F, Kekkarainen T, *et al*. *P16INK4a* is required for *hSNF5* chromatin remodeler-induced cellular senescence in malignant rhabdoid tumor cells. *J Biol Chem* 2004;279:3807–3816.
59. Kia SK, Gorski MM, Giannakopoulos S, *et al*. SWI/SNF mediates polycomb eviction and epigenetic reprogramming of the *INK4b-ARF-INK4a* locus. *Mol Cell Biol* 2008;28:3457–3464.
60. Gresh L, Bourachot B, Reimann A, *et al*. The SWI/SNF chromatin-remodeling complex subunit *SNF5* is essential for hepatocyte differentiation. *EMBO J* 2005;24:3313–3324.
61. Caramel J, Medjkane S, Quignon F, *et al*. The requirement for *SNF5/INI1* in adipocyte differentiation highlights new features of malignant rhabdoid tumors. *Oncogene* 2008;27:2035–2044.
62. Frank SR, Schroeder M, Fernandez P, *et al*. Binding of *c-Myc* to chromatin mediates mitogen-induced acetylation of histone H4 and gene activation. *Genes Dev* 2001;15:2069–2082.
63. Bagnasco L, Tortolina L, Biasotti B, *et al*. Inhibition of a protein-protein interaction between *INI1* and *c-Myc* by small peptidomimetic molecules inspired by *Helix-1* of *c-Myc*: identification of a new target of potential antineoplastic interest. *FASEB J* 2007;21:1256–1263.
64. Bellmeyer A, Kruse J, Lindgren J, *et al*. The protooncogene *c-myc* is an essential regulator of neural crest formation in *xenopus*. *Dev Cell* 2003;4:827–839.
65. Algar EM, Muscat A, Dagar V, *et al*. Imprinted *CDKN1C* is a tumor suppressor in rhabdoid tumor and activated by restoration of *SMARCB1* and histone deacetylase inhibitors. *PLoS ONE* 2009;4:e4482.
66. Tsikitis M, Zhang Z, Edelman W, *et al*. Genetic ablation of *Cyclin D1* abrogates genesis of rhabdoid tumors resulting from *Ini1* loss. *Proc Natl Acad Sci USA* 2005;102:12129–12134.
67. Alarcon-Vargas D, Zhang Z, Agarwal B, *et al*. Targeting cyclin *D1*, a downstream effector of *INI1/hSNF5*, in rhabdoid tumors. *Oncogene* 2006;25:722–734.
68. Xu Y, Tan LJ, Grachtchouk V, *et al*. Receptor-type protein-tyrosine phosphatase- κ regulates epidermal growth factor receptor function. *J Biol Chem* 2005;280:42694–42700.
69. Yajnik V, Paulding C, Sordella R, *et al*. *DOCK4*, a GTPase activator, is disrupted during tumorigenesis. *Cell* 2003;112:673–684.
70. Upadhyay G, Goessling W, North TE, *et al*. Molecular association between β -catenin degradation complex and *Rac* guanine exchange factor *DOCK4* is essential for *Wnt*/ β -catenin signaling. *Oncogene* 2008;27:5845–5855.
71. Rangel J, Nosrati M, Torabian S, *et al*. Osteopontin as a molecular prognostic marker for melanoma. *Cancer* 2008;112:144–150.
72. Shevde LA, Samant RS, Paik JC, *et al*. Osteopontin knockdown suppresses tumorigenicity of human metastatic breast carcinoma, *MDA-MB-435*. *Clin Exp Metastasis* 2006;23:123–133.
73. Kao CL, Chiou SH, Chen YJ, *et al*. Increased expression of osteopontin gene in atypical teratoid/rhabdoid tumor of the central nervous system. *Mod Pathol* 2005;18:769–778.
74. Gao YA, Agnihotri R, Vary CP, *et al*. Expression and characterization of recombinant osteopontin peptides representing matrix metalloproteinase proteolytic fragments. *Matrix Biol* 2004;23:457–466.
75. Abdollahi A, Hlatky L, Huber PE. Endostatin: the logic of antiangiogenic therapy. *Drug Resist Updat* 2005;8:59–74.
76. Herbst RS, Hess KR, Tran HT, *et al*. Phase I study of recombinant human endostatin in patients with advanced solid tumors. *J Clin Oncol* 2002;20:3792–3803.
77. Ramirez-Castillejo C, Sanchez-Sanchez F, Andreu-Agullo C, *et al*. Pigment epithelium-derived factor is a niche signal for neural stem cell renewal. *Nat Neurosci* 2006;9:331–339.
78. Rabinovich GA. Galectin-1 as a potential cancer target. *Br J Cancer* 2005;92:1188–1192.